Yeast Actin with a Mutation in the "Hydrophobic Plug" between Subdomains 3 and 4 ($L_{266}D$) Displays a Cold-sensitive Polymerization Defect

Xin Chen, R. Kimberley Cook, and Peter A. Rubenstein

Department of Biochemistry, University of Iowa College of Medicine, Iowa City, Iowa 52242-1104

Abstract. Holmes et al. (Holmes, K. C., D. Popp, W. Gebhard, and W. Kabsch. 1990. *Nature [Lond.]* 347: 44–49) hypothesized that between subdomains 3 and 4 of actin is a loop of 10 amino acids including a four residue hydrophobic plug that inserts into a hydrophobic pocket formed by two adjacent monomers on the opposing strand thereby stabilizing the F-actin helix. To test this hypothesis we created a mutant yeast actin ($L_{266}D$) by substituting Asp for Leu_{266} in the plug to disrupt this postulated hydrophobic interaction. Haploid cells expressing only this mutant actin were viable with no obvious altered phenotype at temperatures above 20°C but were moderately cold-sensitive for growth compared with wild-type cells. The critical concentration for polymerization increased 10-fold at 4°C compared with wild-type actin. The length of the nucleation phase of polymerization increased as the temperature decreased. At 4°C nucleation was barely detectable. Addition of phalloidin-stabilized F-actin nuclei and phalloidin restored $L_{266}D$ actin's ability to polymerize at 4°C. This mutation also affects the overall rate of elongation during polymerization. Small effects of the mutation were observed on the exchange rate of ATP from G-actin, the G-actin intrinsic ATPase activity, and the activation of myosin S1 ATPase activity. Circular dichroism measurements showed a 15°C decrease in melting temperature for the mutant actin from 57°C to 42°C. Our results are consistent with the model of Holmes et al. (Holmes, K. C., D. Popp, W. Gebhard, and W. Kabsch. 1990. *Nature [Lond.]*. 347:44–49) involving the role of the hydrophobic plug in actin filament stabilization.

A number of groups have used optical reconstruction of high-resolution electron micrographs to study the structure of the F-actin filament (Milligan et al., 1990; Bremer et al., 1991). At this level of resolution, the interstrand contacts which stabilize the actin helix cannot be observed. To date, it has not been possible to crystallize F-actin because actin forms noncrystalline filamentous aggregates or paracrystalline arrays under the conditions normally used for crystallization (Bremer and Aebi, 1992). Thus, there has been no direct experimental investigation of these interstrand actin–actin contacts at atomic resolution. Kabsch et al. (1990) determined the crystal structure of rabbit skeletal muscle G-actin to a resolution of 2.8 A as part of a 1:1 complex with pancreatic DNAse I. They then generated a model of F-actin by placing the monomer in the structure of the actin helix derived from EM measurements and calculating an x-ray fiber diffraction pattern which was fitted to the experimental diffraction pattern by a global search (Holmes et al., 1990). A prominent feature of the monomer structure is a hydrophobic loop encompassing residues 262-272 between subdomains 3 and 4 of the actin molecule. In the monomeric form, this loop extends from the surface of the protein and then hooks back toward the actin in the vicinity of Tyr_{188} (Fig. 1 *A*). Holmes found, however, that he could remodel the loop so that it represented two antiparallel β-strands with a four residue hydrophobic plug in a direction perpendicular to the filament axis (Fig. 1 *B*). The four residue "plug" would then insert into a hydrophobic pocket generated by the interface of two subunits on the opposing strand of the helix (Fig. 1 *C*). Such an interaction would provide a great deal of interstrand stabilization of the actin helix.

Although this is an attractive hypothesis for helix stabilization, no experimental evidence exists for this loop in the extended orientation. To test this hypothesis we have used site-directed mutagenesis to alter a residue in the proposed hydrophobic plug of *S. cerevisiae* actin and have determined the effects of this mutation in vivo and in vitro.

Yeast and rabbit muscle actins are 87% conserved in primary sequence (Gallwitz and Sures, 1980; Ng and Abelson, 1980; Elzinga et al., 1973), and they are highly homologous in the loop region as shown in Fig. 2. The stems of the loop are nearly identical, but the F_{266}-I-G-M- plug of muscle actin is replaced by V_{265}-L-G-L- in yeast. The conserved glycine presumably is necessary to form the turn required for

Address all correspondence to Dr. P. A. Rubenstein, Department of Biochemistry, University of Iowa College of Medicine, Iowa City, IA 52242-1104.

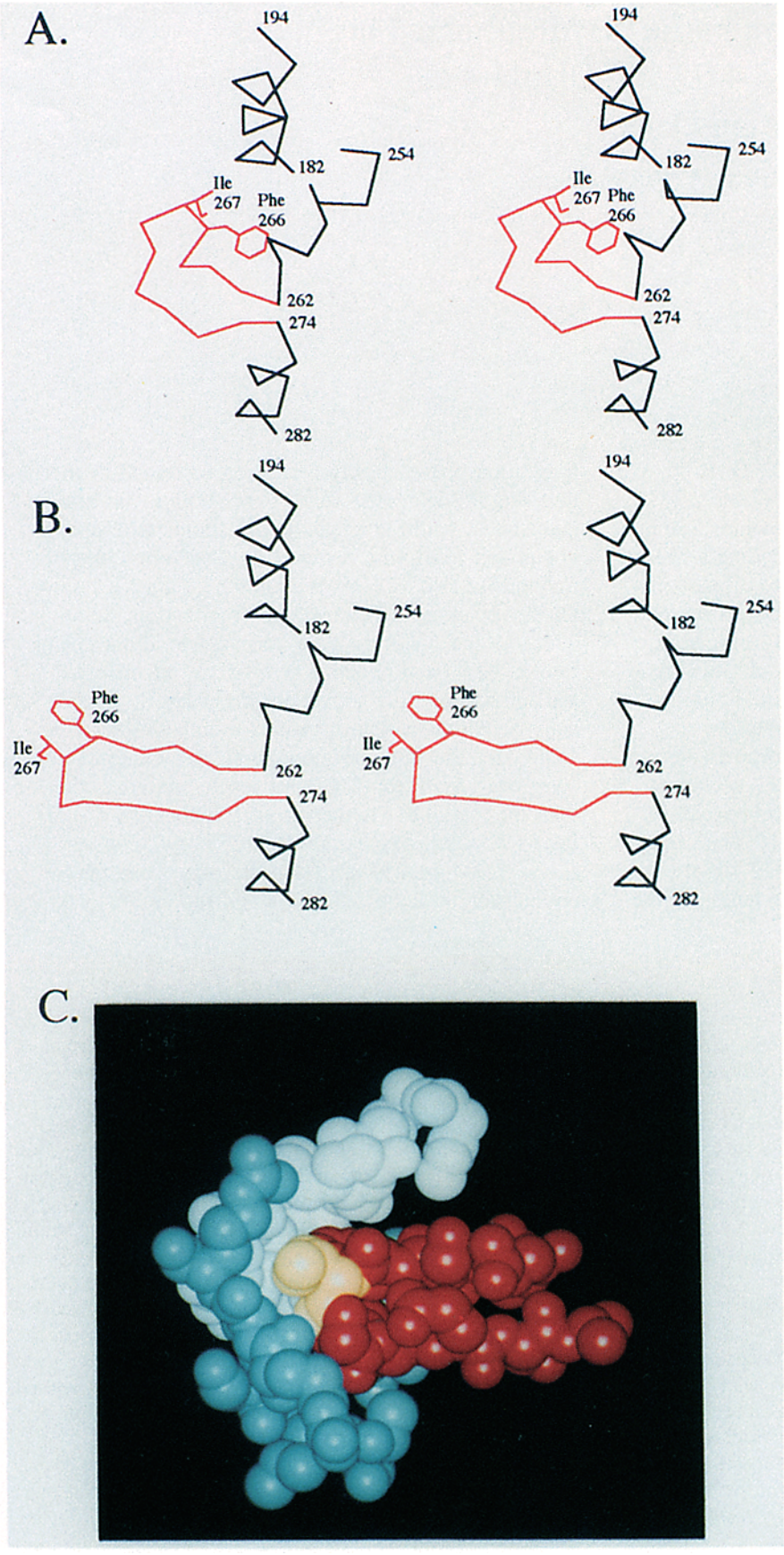

Figure 1. Model of the proposed hydrophobic plug-pocket interaction for rabbit skeletal muscle actin. (*A*) Stereo drawing of the alpha carbon trace showing the conformation of the loop containing the hydrophobic plug (*red*) in the hook conformation as observed in the actin/DNAse I complex. The side chains of F_{266} and I_{267} are also shown. Coordinates used are those deposited by Kabsch et al. (1990) in the Protein Data Bank (Bernstein et al., 1977; Abola et al., 1987). (*B*) Stereo drawing of the α carbon trace showing the conformation of the loop containing the hydrophobic plug (*red*) in the extended conformation as modeled by Holmes et al. (1990). (*C*) Space filling model showing the interaction of the loop (*red*) with a hydrophobic pocket formed at the interface of two actin monomers on the opposite strand of the actin helix (*blue* and *white*). Ile_{267} in muscle actin which corresponds to the position of the $L_{266}D$ mutation in yeast actin, is shown in yellow. Coordinates used for *B* and *C* are those of Lorenz et al. (1993).

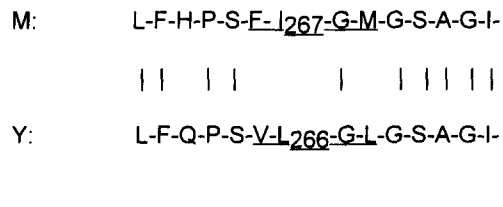

Figure 2. Sequences of the loop between actin subdomains 3 and 4 containing the hydrophobic plug for the wild-type and mutant actin used in this study. The four residue hydrophobic plug is underlined, and the vertical lines indicate the conservation of residues between yeast and rabbit skeletal muscle actins in this region. The double lines indicates the site of the $L_{266}D$ mutation. *M*, rabbit skeletal muscle; *Y*, yeast wild-type actin; *$L_{266}D$*, substitution of Leu_{266} with Asp.

loop formation. Holmes predicted that elimination of the plug–pocket interaction would severely affect the ability of actin to form stable filaments. In this paper, we report the results of inserting into the plug a hydrophilic residue, aspartic acid, in place of Leu_{266}.

Materials and Methods

The site-directed mutagenesis kit, [α-^{35}S]-Adenosine-5′-thiotriphosphate, >1,000 Ci/mmole, and [γ-^{32}P]ATP, 6,000 Ci/mmole were purchased from Amersham Corp. (Arlington Heights, IL). Rhodamine-phalloidin was purchased from Molecular Probes (Eugene, OR). DNAse I was obtained from Worthington Biochemicals Corp. (Freehold, NJ). The phagemid pGEM 3Z(−) was obtained from Promega Biotec (Madison, WI). The Sequenase Version 2.0 DNA sequencing kit was purchased from U.S. Biochemical Corp. (Cleveland, OH). Phalloidin was obtained from Sigma Chemical Co. (St. Louis, MO). The oligodeoxynucleotide used for site-directed mutagenesis was synthesized in the DNA Core Facility at the University of Iowa (Iowa City, IA). The S1 fragment of rabbit skeletal muscle myosin was prepared by the method of Weeds and Taylor (1975). Rabbit skeletal muscle actin was prepared from acetone powder (Pardee and Spudich, 1982) by DNAse I chromatography coupled with anion exchange chromatography according to Cook et al. (1993). The SLM 4800 fluorescence spectrometer and the AVIV 62 DS spectropolarimeter used in this work are part of the Protein Structure Facility in the College of Medicine at the University of Iowa.

Plasmid Manipulations and Mutagenesis

Procedures for manipulating plasmids are those described in Ausubel (1987). Single-stranded DNA was generated from the phagemid pGEM-3Z(−) into which the yeast actin coding sequence and the yeast actin promoter had been inserted between the EcoRI and BamHI sites in the polylinker. The single stranded DNA was then used as a template for site-directed mutagenesis together with the oligodeoxynucleotide 5′-TTCCATCCTTCTGTTGATGGTTTGGAATCTGCC-3′ to generate the $L_{266}D$ mutant actin coding sequence in which Leu_{266} is converted to aspartic acid. Following the number system of Wertman et al. (1992), we have named this actin allele actl-137 ($L_{266}D$). The resulting mutant DNA was sequenced to verify the desired mutation. An expression vector, pCEN-LD, was constructed by substituting the EcoRI–HindIII fragment containing the mutant sequence for the homologous wild-type sequence contained in the centromeric yeast vector pCEN-WN which carries the entire yeast actin coding sequence adjacent to the yeast actin promoter (Cook et al., 1991).

The plasmid was used to generate diploid cells carrying both the wild-type and mutant actin coding sequences and haploid cells containing the mutant actin coding sequence as the only active actin coding sequence in the cell (Cook et al., 1991). The plasmid was reisolated from the yeast and sequenced to verify that the transformed cells contained the desired mutation.

Yeast Strains and Manipulations

S. cerevisiae strain TDyDD was a gift of D. Shortle (Johns Hopkins University, Baltimore, MD). It is a diploid cell in which one actin allele has been partially deleted and marked with LEU2+ (Cook et al., 1991). Strains TDyLD and TDyWN are haploid derivatives of TDyDD containing the chromosome carrying the interrupted actin gene and the plasmid pCEN-LD carrying the $L_{266}D$ actin coding sequence or pCEN-WN carrying the wild-type actin coding region respectively. Yeast were grown in YPD (1% yeast extract, 2% peptone, 2% glucose) or synthetic defined medium (Sherman, 1990). Yeast was transformed using a modification of the method of Ito et al. (1983).

Purification of Yeast Wild-type and $L_{266}D$ Actins

Wild-type yeast actin was purified in an active form using the DNAse I agarose procedure of Cook and Rubenstein (1992). The same procedure was used to obtain monomeric $L_{266}D$ actin. However, because this actin has a cold-sensitive polymerization defect, the actin was polymerized and the F-actin collected by centrifugation at 25°C instead of 4°C as previously published.

Actin Polymerization Assays

Actin polymerization was carried out in F-buffer (10 mM Tris-HCl, pH 7.5, 0.2 mM $CaCl_2$, 0.2 mM ATP, 2 mM $MgCl_2$, 50 mM KCl, and 0.1 mM DTT). Polymerization was followed by centrifugation or by light scattering. For the sedimentation assay at temperatures below 20°C, the actin was polymerized at the desired temperature for 15 h and centrifuged for 1 h at the same temperature at 60,000 rpm in a table ultracentrifuge (TL100; Beckman Instruments, Palo Alto, CA) using a TLA 100.2 rotor. The protein concentration of the supernate was then determined using the Pierce BCA assay. For temperatures above 20°C, polymerization was carried out for 3 h. Subsequent experiments using light scattering showed that this time was sufficient for complete polymerization.

In the light scattering assay, the sample was equilibrated in G buffer (10 mM Tris-HCl, pH 7.5, 0.2 mM $CaCl_2$, 0.2 mM ATP, and 0.1 mM DTT) at the appropriate temperature for 30 min in a thermostated cuvette chamber in an SLM 4800 fluorescence spectrometer with excitation and emission wavelengths both at 360 nm. The microcuvette had cross-sectional dimensions of 3 mm × 3 mm. Polymerization was initiated by adding KCl and $MgCl_2$ to final concentrations of 50 and 2 mM, respectively, and the change in light scattering recorded as a function of time. Alternatively, polymerization was induced by the addition of phalloidin-stabilized yeast wild-type F-actin seeds at a concentration of 0.025 or 0.05 μM actin. Seeds were prepared by incubating 10 μM F-actin with 0.9 μM phalloidin followed by vigorous vortexing of the resulting filaments before the addition to the G-actin. After establishing the baseline, polymerization was induced as described above. For determining polymerization elongation rates, increasing amounts of wild-type or mutant G-actin were combined in G buffer with 0.05 μM phalloidin-stabilized wild-type actin seeds, and the initial rate of elongation determined at each actin concentration following introduction of 2 mM $MgCl_2$ and 50 mM KCl to induce polymerization.

In the light scattering experiments just described, we often observed one or several large sharp symmetrical peaks during the first 50 s following mixing of the samples and placing the cuvette in the fluorimeter. These mixing artifacts appeared randomly with all types of actin used and seemed more prevalent at colder temperatures. We have manually smoothed the tracings shown in Figs. 5, 6, and 9 to remove these spikes.

The critical concentration (*Cc*)[1] for actin association was also determined using light scattering. For measurements at 25°C, F-actin was diluted to the appropriate concentration in F buffer at the appropriate temperature for 3 h, and the change in light scattering was determined. For measurements at 10°C and 4°C, the incubation time was extended to 24 h. For every concentration tested, the light scattering of an equivalent amount of G-actin in G buffer was determined and deducted as a baseline value.

Actin–ATP and Actin–Myosin S1 Interactions

The rate of dissociation of ATP from actin was determined according to Mockrin and Korn (1980) using radiolabeled ATP as a probe. The intrinsic

1. *Abbreviations used in this paper*: Cc, critical concentration; Tm, melting temperature.

rate of ATP hydrolysis by G-actin was determined by a combination of the methods of Haarer et al. (1990) and Tobacman and Korn (1982). The activation of myosin S1 ATPase activity by actin was measured according to Cook et al. (1992) based on the procedure of Spudich (1974).

Electron Microscopy

Actin filaments, negatively stained by 1.5% uranyl acetate, were examined by EM of samples on carbon-coated Formvar grids using an electron microscope (7000; Hitachi Instruments, Inc., San Jose, CA). This work was performed in the Central Electron Microscope Facility at the University of Iowa.

Staining with Rhodamine Phalloidin and Calcafluor

Yeast cells were stained with rhodamine phalloidin or Calcafluor, and fluorescence micrographs were obtained on a microscope (Carl Zeiss, Oberkochen, Germany) using TMAX 400 film according to the procedure of Pringle et al. (1991).

Actin Filament Viscometry

The viscosity of F-actin solutions was determined with a falling ball viscometer (Cooper, 1992) using a path length of 7–9 cm and an angle of inclination of 12°. Actin was polymerized at a given temperature for a specific period of time after which it was drawn into the microcapillary pipette and incubated for an additional 1/2 h at the same temperature. Measurements were obtained in duplicate or triplicate on a number of different actin preparations with similar results obtained from different preparations of the same actin.

Circular Dichroism Measurements

For these experiments, the 1.4 μM actin in a buffer containing 2 mM Hepes, pH 8.0, 0.2 mM $CaCl_2$, 0.2 mM ATP, and 0.5 mM β-mercaptoethanol was placed in a 3-ml stoppered quartz cuvette with a path length of 1 cm. Measurements were performed on an AVIV 62 DS spectropolarimeter equipped with a thermoelectric temperature controller and an immersible thermocouple, accurate to ±0.4°C, for direct monitoring of the temperature of the sample. The sample was heated at a constant rate of 1°C/min over a temperature range extending from 0°C to 80°C with constant stirring of the sample over the entire range tested. Changes in ellipticity were monitored at 222 nm. Buffer alone showed no change in ellipticity with temperature and was therefore ignored during data analysis. Data were analyzed using a Macintosh version of a nonlinear least-squares fitting program developed by Johnson and Frasier (1985). Data were processed and presented using Cricket Graph (Computer Associates International, Inc., West Conshohocken, PA).

Results

In Vivo Studies with the $L_{266}D$ Mutant Actin

When we transformed the yeast with the plasmid containing the actin coding sequence carrying the Leu_{266}→Asp mutation, we obtained transformants with the same frequency as when we used a plasmid containing the wild-type actin coding sequence. Dissection of tetrads following the induction of these cells to undergo meiosis allowed us to readily obtain viable haploid cells (TDyLD) in which the $L_{266}D$ actin, synthesized from the plasmid-borne coding sequence, was the only actin in the cell. Furthermore, these cells appeared to grow on YPD agar plates at temperatures ranging from 20°C to 37°C as well as wild-type cells. By microscopic examination, the morphology and size of the $L_{266}D$ cells also appeared normal. Thus, contrary to our prediction based on the Holmes model, introduction of an acidic residue in the hydrophobic plug apparently did not significantly destabilize the actin helix in vivo under the conditions tested.

It is difficult to obtain quantitative differences in growth of yeast on agar plates. We thus measured the generation times for cells expressing $L_{266}D$ actin versus wild-type actin at various temperatures in liquid culture. Table I shows no difference in the ratio of growth rates of the mutant and wild-type cells between 20°C and 37°C. However, as the temperature decreased below 20°C the ratio of the growth rates of these two cultures increased reaching a value of about 1.4 at 10°C. Thus, the $L_{266}D$ mutation causes a non-lethal cold-sensitive phenotype. $L_{266}D$ cells grown at 10°C were stained with rhodamine phalloidin to visualize F-actin and with Calcafluor to visualize the pattern of chitin deposition. No differences were observed between the cells carrying the wild-type and $L_{266}D$ actins (data not shown).

Finally, we examined the ability of these cells to grow on agar in hyperosmolar medium. Chowdhury et al. (1992) recently reported that introduction of yeast to hyperosmolar medium causes a temporary cessation of growth and a gross fragmentation and rearrangement of the actin cytoskeleton. Under these conditions, cells containing certain mutant actins could not grow. If nucleation of filaments and their subsequent assembly in vivo was affected by the $L_{266}D$ mutation in a manner suggested by the Holmes model, proper reassembly of the cytoskeleton might be compromised in hyperosmolar medium, especially at lower temperatures where the defect is most evident. However, relative to wild-type cells, $L_{266}D$ cells grew between 10°C and 30°C to the same extent on agar in hyperosmolar medium (YPD containing 1.2 M KCl or 1.8 M sorbitol) as they did on normal YPD plates.

Polymerization of the $L_{266}D$ Mutant Actin In Vitro

We then purified the actin for biochemical studies in vitro. The $L_{266}D$ actin bound to a DNAseI affinity column, a step in the purification procedure, indicating that the mutation produced no gross distortion of the monomeric structure of actin. Repeated attempts to polymerize the actin by incubation at 4°C overnight in F buffer after incubation at room temperature for 30 min were unsuccessful. However, polymerization of the $L_{266}D$ actin occurred readily when the actin was incubated in F buffer for 2 h at 25°C. Thus the hydrophobic plug mutation resulted in a cold-sensitive polymerization defect.

To further characterize the effects of temperature on the polymerization of $L_{266}D$ actin, we measured the centrifugation properties of the actin as a function of temperature (Fig. 3). For these experiments, the starting actin concentration was 3 mg/ml (70 μM). Under the conditions of the assay, the amount of wild-type actin pelleted remained constant over

Table I. Doubling Times of TDyLD and TDyWN Cells at Different Temperatures

	9°C	10.5°C	15°C	20°C	30°C	37°C
TDyLD (h)	33	22.5	8.7	4.9	2.1	4.7
TDyWN (h)	22.7	17.2	7.1	4.9	2.1	4.7
LD/WN	1.5	1.4	1.2	1.0	1.0	1.0

Shown are the doubling times and the ratios of the doubling times for the TDyLD and TDyWN yeast strains grown in YPD medium. Growth at temperatures between 9°C and 20°C were monitored with cultures in a revolving drum. Growth at higher temperatures was monitored using a shaking platform. Each doubling time represents the average of three parallel cultures grown simultaneously. For each temperature, growth of both cell types were monitored concurrently. LD/WN is the ratio of the doubling times.

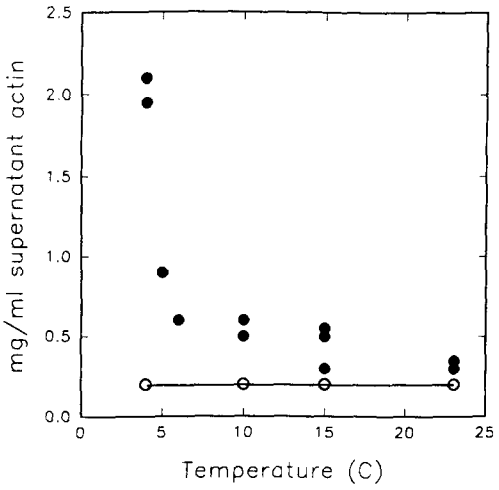

Figure 3. Sedimentation of wild type and F-actin as a function of temperature. The vertical axis represents the concentration of actin remaining in the supernatant. (○) wild-type actin; (●) $L_{266}D$ actin.

a temperature range from 4°C to 22°C. For the $L_{266}D$ actin, the amount of protein remaining in the supernate at 22°C was about twice that of the wild-type protein. As the temperature decreased to 10°C, the actin remaining in the supernate increased from 0.2 mg/ml (4.6 μM) to ~0.5 mg/ml (11.6 μM). As cooling continued to 4°C, there was a marked increase in supernatant actin to a level of about 2 mg/ml (46.5 μM), suggesting the occurrence of a cooperative transition.

To begin to determine the basis for this unusual centrifugation behavior of the $L_{266}D$ actin, we examined preparations of the protein by EM after the addition of 2 mM $MgCl_2$ and 50 mM KCl. Fig. 4 *C* shows that the mutant actin forms normal looking filaments at room temperature. At 10°C stringy aggregates were observed, but defined filaments were not detected. When polymerization was carried out in the presence of 0.05 μM phalloidin stabilized wild-type actin seeds, we sometimes detected normal appearing filaments (Fig. 4 *B*). More often we observed disordered or broken filamentous-like structures in which actin subunits were clearly visible suggesting that the filaments may be breaking apart during preparation of the EM specimens. This may have been due in part to the fact that for the 10°C samples, we polymerized the actin at 0.8 mg/ml (18.6 μM) and then diluted the sample to 0.3 mg/ml (7 μM) with gentle pipetting just before application of the sample to the grid. We did not convincingly observe structures that would have indicated an unwinding of the F-actin helix into single strands. At 4°C, where little if any actin pelleted in the centrifugation assay at actin concentrations below 2 mg/ml (46.5 μM), no filaments were seen either with 11 μM pure mutant actin or with mutant actin in the presence of wild-type actin seeds (data not shown). However, if equimolar amounts of phalloidin and $L_{266}D$ actin were mixed in the presence of wild-type actin seeds, normal looking filaments were readily apparent (Fig. 4 *A*). These results suggest that the $L_{266}D$ mutation results in a pronounced decrease in the ability of the actin to nucleate filament assembly and a decrease in the stability of the filament once it is formed. The ability of the mutant actin to generate normal filaments in the presence of seeds and phalloidin at 4°C demonstrates that the alterations caused by the mutation do not result in structural changes that affect the addition of monomers to a filament per se.

We used light scattering to determine the effect of the $L_{266}D$ mutation on the kinetics of association of the actin monomers at 25°C, 10°C, and 4°C. As shown in Fig. 5 *A*, at 25°C there is a significant lag in the onset of the elongation phase compared with that observed with wild-type yeast actin. At 10°C, using 0.8 mg/ml (18.6 μM) of actin, the 1,500-s lag in the onset of monomer association was even more pronounced when compared with that seen with wild-type actin (Fig. 5 *B*). At 4°C no increase in light scattering was observed for at least 6,000 s after the addition of F-salts although wild-type actin readily polymerized under these conditions (Fig. 5 *C*).

If the $L_{266}D$ mutation affected nucleation of filaments, addition of preformed F-actin nuclei should decrease the lag phase of the observed light scattering curve. The addition of phalloidin-stabilized wild-type actin nuclei at 10°C to a concentration of 0.025 to 0.05 μM increased the rate at which the $L_{266}D$ actin monomers polymerized (Fig. 6 *A*) although nucleation and elongation were still slower than with wild-type actin. We observed a similar effect at 4°C where, in the absence of added nuclei, polymerization was virtually

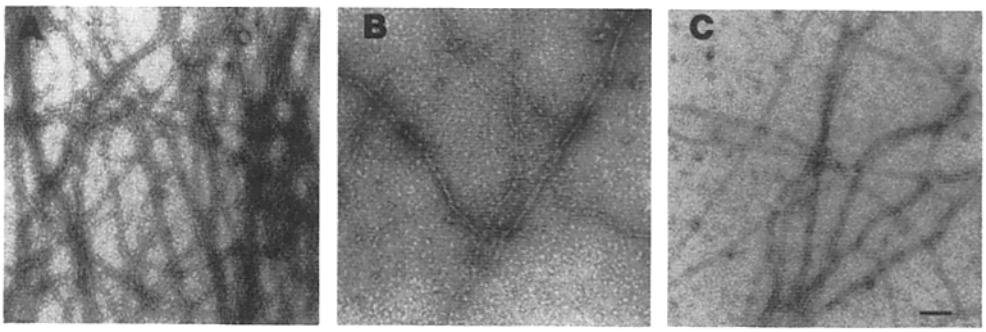

Figure 4. EM of yeast $L_{266}D$ actin at different temperatures. Mutant G-actin was polymerized in F-buffer for 1 h at the temperature indicated and viewed by negative staining with uranyl acetate. (*A*) 7 μM actin was polymerized at 4°C in the presence of equimolar phalloidin and wild type actin seeds. (*B*) 18.6 μM actin was polymerized at 10°C in the presence of wild-type actin seeds and diluted to 7 μM in F buffer before application to the grid. (*C*) 7 μM actin was polymerized at room temperature. Bar, 0.1 μm.

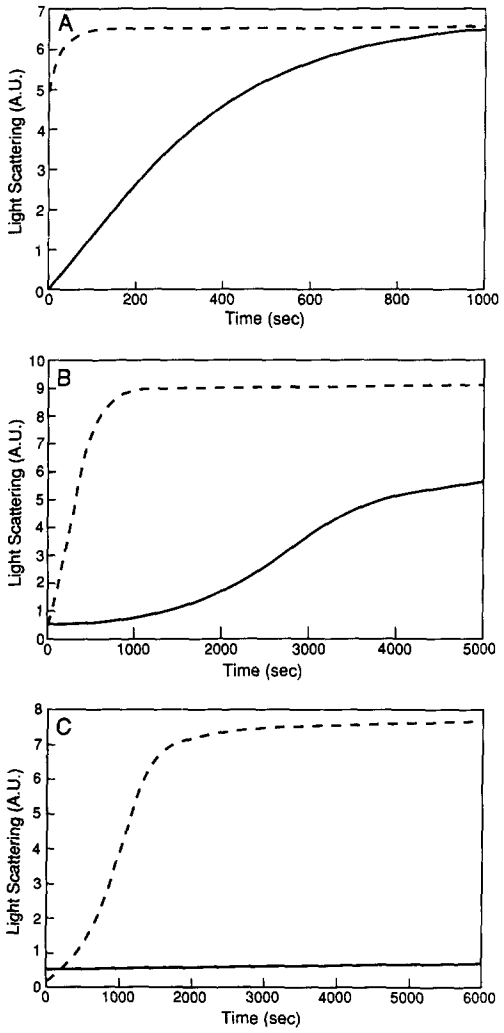

Figure 5. Effects of temperature on the polymerization of $L_{266}D$ actin. Polymerization of yeast wild-type and $L_{266}D$-actins was followed as a function of time using a light scattering assay. For each experiment, the actin concentration was 18.6 μM. (———) $L_{266}D$ actin; (------) wild-type actin. (*A*) 25°C; (*B*) 10°C; (*C*) 4°C.

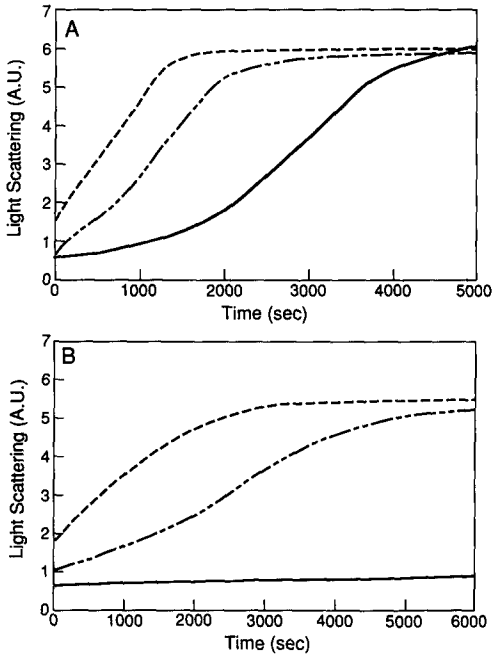

Figure 6. The effects of added phalloidin-stabilized actin nuclei on the polymerization of $L_{266}D$ actin at different temperatures. Actin nuclei were added prior to the initiation of polymerization as indicated. For each experiment, the actin concentration was 18.6 μM. (———) $L_{266}D$ actin without nuclei; (------) $L_{266}D$ actin with 0.05 μM added nuclei; (———-———) $L_{266}D$ actin with 0.025 μM added nuclei. (*A*) 10°C; (*B*) 4°C.

nonexistent (Fig. 6 *B*). However, at this temperature, due to the effect of the mutation on the ability of the actin to form stable filaments, we propose that this nucleation produced amorphous aggregates instead of filaments shown in Fig. 4.

We next determined the effect of the $L_{266}D$ mutation on the elongation rate of actin polymerization by measuring the rate at which different concentrations of actin polymerized at 22°C and 10°C in the presence of a constant amount of stabilized F-actin seeds. Fig. 7 shows that at both temperatures, the elongation rate for the $L_{266}D$ actin was two to three times slower than that observed with the wild-type actin. A similar difference was observed at 4°C. The failure to observe recognizable filaments under these conditions at 4°C under the electron microscope made interpretation of this last piece of data difficult. However, the ability of the $L_{266}D$ actin to form filaments in the presence of phalloidin at 4°C suggests that the seed-induced increase in light scattering at 4°C reflects an actin–actin association occurring in the normal polymerization process. In all light scattering experiments, no increase in light scattering was observed with the seeds alone.

Having demonstrated an effect of the mutation on both filament nucleation and elongation, we next determined the Cc for association at temperatures ranging from 4°C to 25°C using a light scattering assay which is largely independent of filament length (Tobacman and Korn, 1982). The results with $L_{266}D$ actin are shown in Fig. 8, and the critical concentrations for both mutant and wild-type actins are shown in Table II. The apparent Cc at 25°C for the $L_{266}D$ mutant (1.2 μM) was two to three times that determined for wild-type actin (0.4 μM). At 10°C and 4°C, the value for Cc for the $L_{266}D$ actin increased to 6.5 and 11 μM, respectively, compared with 0.65 and 1.7 μM for the wild-type actin at the same temperatures. This behavior mirrored that observed in the centrifugation assay.

Effect of the $L_{266}D$ Mutation on Filament Viscosity

We next examined the viscosity of the $L_{266}D$ actin under various conditions using falling ball viscometry. The results are shown in Table III. At room temperature, the viscosities observed for both wild-type and $L_{266}D$ actin were similar, although we consistently observed that the viscosity of $L_{266}D$ actin was actually slightly higher than that of the wild-type actin. At 10°C, the viscosity of the mutant actin was about one-fourth that of the wild type. Addition of seeds produced no increase in the viscosity of the mutant. However, when polymerization of both mutant and wild-type ac-

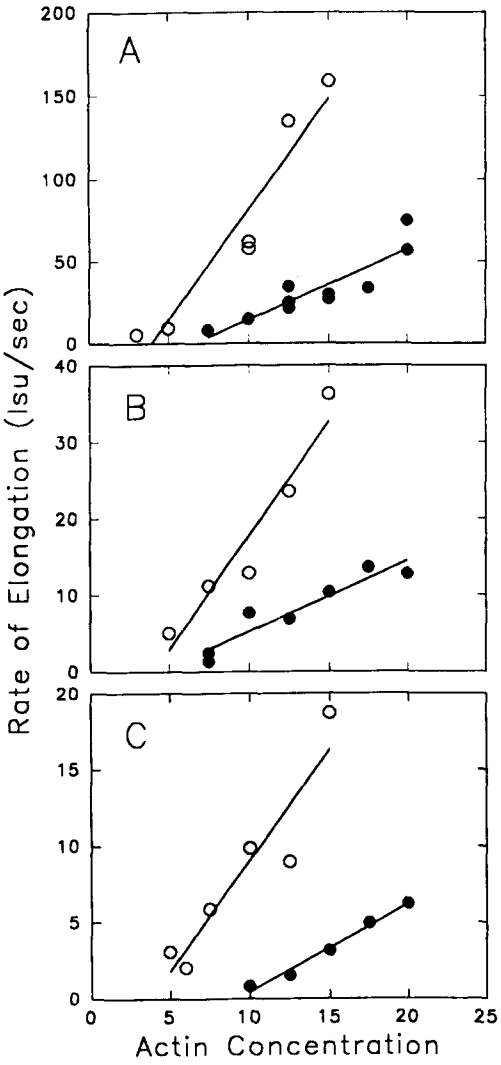

Figure 7. Elongation rates of $L_{266}D$ and wild-type actins as a function of temperature. The initials rates of polymerization of wild-type (○) and $L_{266}D$ (●) actins in the presence of 0.05 μM wild-type actin seeds were measured and the elongation rates were plotted as a function of actin concentration. (*lsu*) light scattering units. (*A*) 23°C; (*B*) 10°C; (*C*) 4°C.

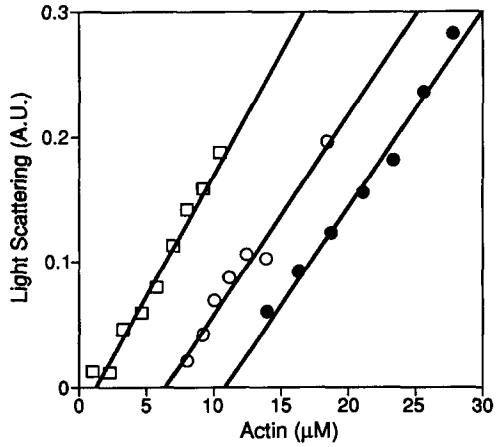

Figure 8. The Cc of $L_{266}D$ actin as a function of temperature. Values were determined by light scattering. (□) 25°C; (○) 10°C; (●) 4°C.

Table II. Critical Concentration for Polymerization of Wild-type and $L_{266}D$ Actins

Temperature	Wild-type actins	$L_{266}D$ actins
	(μM)	(μM)
23°C	0.4	1.2
10°C	0.7	6.5
4°C	1.7	11

Table III. Viscosity Measurements of Wild-type and $L_{266}D$ Actins at Different Temperatures

Temperature	4°C	10°C	23°C
Wild type	0.8 ± 0.1*	3.0 ± 0	1.7 ± 0
	3.4 ± 0.1		
$L_{266}D$	0.9 ± 0.1‡	0.7 ± 0.1	2.3 ± 0.1
$L_{266}D$ plus seeds	1.4 ± 0.1‡	0.8 ± 0.1	n.d.§
Wild-type plus phalloidin	45 ± 8	39 ± 4	n.d.
$L_{266}D$ plus phalloidin	38 ± 5	45 ± 5	n.d.

Values shown for the $L_{266}D$ actin are derived from data shown in Fig. 8. Values for wild-type actin were obtained by carrying out a similar set of experiments with this actin.
Values are expressed in s/cm. All concentrations are 11.6 μM (0.5 mg/ml) except as noted.
* 4.7 μM (0.2 mg/ml)
‡ 18.6 μM (0.8 mg/ml)
§ n.d., not done

tins were carried out in the presence of phalloidin, both actins showed comparable viscosities indicating the phalloidin stabilized the filament structures of both actins to the same extent.

At 4°C where polymerization is undetectable by light scattering, 18.6 μM $L_{266}D$ actin had about the same viscosity as 4.6 μM wild-type actin and only about one-fifth of the viscosity observed with 11.6 μM wild-type actin. This $L_{266}D$ actin viscosity is probably attributable in large part to simply the high protein concentration present and not to the presence of filaments or aggregates. Addition of seeds to this actin produced a slight increase in viscosity which may reflect the aggregation observed by EM and light scattering. When phalloidin was added, however, a massive increase in viscosity was observed such that the viscosity of the mutant and wild-type actins were now equal. These results, together with the EM data at 4°C, confirm that the $L_{266}D$ mutation produces a temperature-sensitive instability in the filament that can be overcome by the stabilizing influence of the added phalloidin to produce a normal actin filament structure.

Effect of the $L_{266}D$ Mutation on the DNAse I-induced Depolymerization of Actin

To investigate further whether the $L_{266}D$ mutation destabilizes the actin filament, we measured the effect of DNAse I on these filaments. Since DNAse I binds to monomers rapidly, its presence causes a gradual depolymerization of the actin filaments. If the $L_{266}D$ F-actin is less stable than wild-type F-actin, it should depolymerize more rapidly in the presence of DNAse I. Fig. 9 demonstrates a faster depolymerization of the $L_{266}D$ actin than wild-type actin in the presence of DNAseI. In a control experiment in which buffer

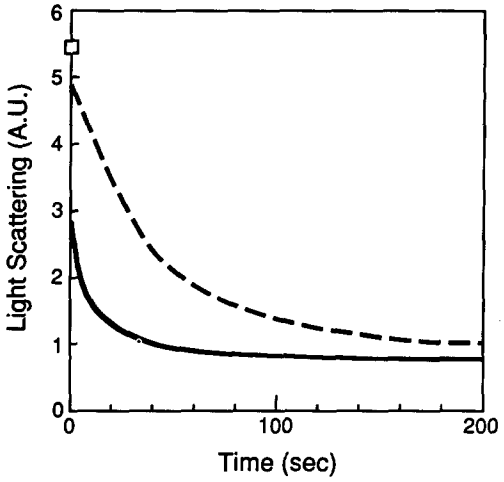

Figure 9. Effect of DNAse I on the stability of yeast wild type and $L_{266}D$ F-actin filaments. F-actin (23 μM) and DNAse I were combined in equimolar amounts in F buffer and the light scattering of the solution monitored at 25°C as a function of time after addition of the DNAse I. The square on the vertical axis denotes the starting light scattering value for both actins. (——) $L_{266}D$ actin; (------) wild-type actin.

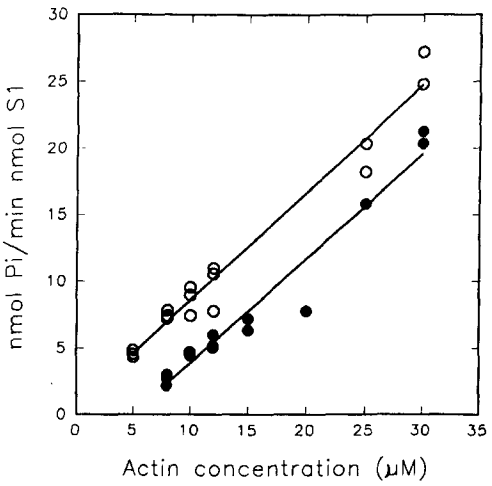

Figure 10. Activation of skeletal muscle myosin S1 ATPase activity by yeast wild-type and $L_{266}D$ actins. Assays were performed at 22°C using 5–30 μM actin, 1.5 μM S1, and 1.5 mM ATP. (o) Wild-type actin; (•) $L_{266}D$ actin.

only was added instead of DNAse I, no decrease in light scattering was observed with either actin. The observed filament instability may be caused by a faster off rate of the $L_{266}D$ monomer from the filament ends compared with a wild-type actin filament. Alternatively, the gentle mixing of the actin and DNAse solutions with a Pasteur pipette at the beginning of the experiment may have resulted in a larger number of filament ends causing the more rapid depolymerization observed. Although we cannot presently distinguish between these possibilities, the result supports our assertion that the $L_{266}D$ actin filament is less stable in solution compared with its wild-type counterpart.

Effect of the $L_{266}D$ Mutation on the Activation of Myosin S1 ATPase Activity

Although at temperatures ≥20°C, $L_{266}D$ filaments appeared normal by EM, the mutation may have caused a change in the surface topology of the filament leading to an altered ability to interact with various F-actin binding proteins. We therefore assessed the relative abilities of the $L_{266}D$ and wild-type yeast actins to activate the skeletal muscle myosin S1 ATPase activity. If an alteration in surface topology interfered with the normal actin-myosin interaction, curves of myosin ATPase activity versus actin concentration should have different slopes. As shown in Fig. 10, the slopes were the same although the curve for $L_{266}D$ actin was laterally displaced indicating that the amount of functional $L_{266}D$ F-actin per total actin added was less than when a comparable amount of wild-type actin was added. This is the result expected if the mutation affected Cc for the actin but did not significantly affect its filamentous structure.

Effect of the $L_{266}D$ Mutation on Properties of G Actin

According to the Holmes model, a change in the hydrophobic plug such as the $L_{266}D$ mutation should affect filament assembly much more than the properties of the actin monomer. The ability to purify $L_{266}D$ actin using DNAseI agarose affinity chromatography shows that the mutation does not cause a large-scale alteration of G-actin structure. To further investigate the effect of the $L_{266}D$ mutation on G-actin structure, we studied the rate at which bound radiolabeled ATP dissociated from wild-type and $L_{266}D$ G-actins in the presence of added unlabeled ATP. ATP binds to actin within a cleft separating subdomains 1 and 2 from 3 and 4 using binding sites on both sides of the cleft (Kabsch et al., 1990). An alteration which affects the spatial relationship of these domains should affect ATP binding. Although the mutation affected polymerization at room temperature, Table IV shows that at room temperature the ATP exchange rates for wild type and $L_{266}D$ actins were identical. However, at 4°C, the exchange rate for the $L_{266}D$ actin was only half as fast as for the wild-type actin indicating that the mutation causes a small but significant conformational change of the monomer at this lower temperature resulting in perhaps a more rigid structure.

As another probe of the conformation of the actin monomer, we compared the intrinsic ATPase activities of wild-type and $L_{266}D$ G-actin. Fig. 11 shows that the wild-type actin hydrolyzed ATP at twice the rate observed for the mutant protein, indicating in this case that at 30°C, the mutation induces a small conformational change in the monomer.

As a final probe of the conformation of the $L_{266}D$ actin monomer, we determined the thermostability of the wild-

Table IV. The ATP Exchange Rates of Yeast Wild-type and $L_{266}D$ Actins at 22°C and 4°C

°C	WT (s-1 × 10^3)	$L_{266}D$ (s-1 × 10^3)
22	5.8 ± 1.1 (n = 8)	5.7 ± 1.0 (n = 4)
4	2.1 ± 0.4 (n = 3)	1.2 ± 0.2 (n = 4)

The data is presented as the rate ± SD. n, the number of repetitions used in each determination.

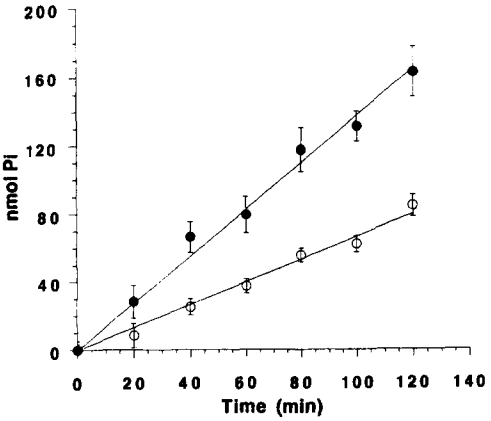

Figure 11. Intrinsic ATPase activity of yeast wild type and $L_{266}D$ actins. The experiment was performed three times at 30°C with essentially the same results. (●) Wild-type actin; (○) $L_{266}D$ actin.

type and mutant actins by monitoring their ellipticity at 222 nm as a function of temperature. Fig. 12 shows that the mutation causes a 15°C decrease in the melting temperature of the mutant actin (42°C) in comparison with the wild type (57°C) yeast or skeletal muscle (57°C) actins indicating perhaps a more flexible structure that is more susceptible to thermal denaturation. Our value for rabbit skeletal muscle actin is identical to that reported previously under the same buffer conditions (Strzelecka-Golaszewska et al., 1985; Bertazzon et al., 1990).

Discussion

The model of Holmes et al. for F-actin (1990) predicts cross-strand stabilization resulting from the insertion of a hydrophobic plug consisting of residues 265–268 of yeast actin into a hydrophobic pocket formed by the interface of two subunits on the opposing strand. Hydrophobic interactions are cold sensitive (Baldwin, 1986; Privalov and Gill, 1988); that is, they weaken as the temperature decreases. In the case of the mutant actin, insertion of Asp_{266} in place of leucine might destabilize this interaction although, at room temperature, not enough to drastically affect F-actin stability. As the temperature decreases, the disruption in the remaining hydrophobic interactions would increase until the disruption prevented formation of a stable polymer.

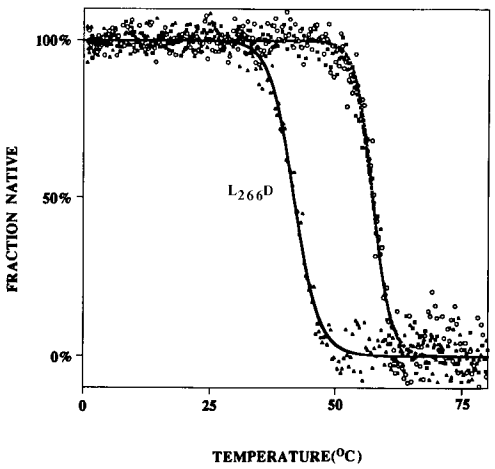

Figure 12. Thermal denaturation of $L_{266}D$, yeast wild type, and rabbit skeletal muscle actins. The ellipticity of each of the actins at 222 nm was monitored as a function of temperature. The lines shown represent the best fit of the data using a nonlinear least-squares analysis (Materials and Methods). The melting curves were transformed to reflect the percent of the protein remaining in the native conformation at each temperature. The left curve is that of $L_{266}D$ actin. The right curve is actually the curves for yeast wild-type and rabbit skeletal muscle actins which overlap.

Our results are generally consistent with the predictions of this model. As judged by kinetic and viscosity measurements, both the rate and extent of the polymerization of the $L_{266}D$ mutant actin are drastically affected, especially at lower temperatures. Compared with wild-type actin, more mutant actin is needed to activate myosin S1 ATPase at 25°C although the catalytic efficiency of this actin is the same as that of wild-type actin once a threshold level of actin has been exceeded. The mutation does affect properties of the monomer in comparison to wild-type actin. This is evidenced by a lower intrinsic ATPase activity at 30°C, a slower rate of ATP exchange at 4°C, and a lower melting temperature. Structural alterations resulting in the lowered thermal stability may not be relavent to the effects of the mutation on polymerization since the melting temperature (Tm) is outside the temperature range used in the other studies reported here. Although these effects seem much smaller than would be needed to explain the severe effects of the mutation on the polymerization properties of actin, it is still possible that an alteration in the alignment of the four subdomains relative to one another might be partly responsible for the abnormal polymerization we observed.

Nucleation of filament formation is thought to occur by the slow association of two monomers followed by stabilization of the complex by a faster addition of a third monomer (Frieden, 1982; Zimmerle and Frieden, 1988). The filament then elongates from this complex. Partial disruption of the plug–pocket interaction in this complex would have a drastic effect on the stability of the nucleus since this hydrophobic interaction would constitute a major component of the intersubunit interactions. Our results demonstrate a large effect of the mutation on nucleation in agreement with this prediction.

This disruption would, to a lesser degree, also affect filament elongation. The addition of each monomer to the growing filament would be compromised. However, once the filament formed, the sum of all interstrand interactions along the filament would be great enough to partially stabilize the actin helix. Although our studies show that at every temperature examined, the elongation rate for the mutant actin was slower than for the wild-type actin, the ratio of elongation rates of these actins was identical. This lack of cold sensitivity suggests that the effect of the mutation on elongation may be due more to a small conformation change in the entire actin structure rather than a disruption of the hydrophobic plug–pocket interaction.

Holmes' model predicts that the residues making up the hydrophobic loop can exist in two conformations. In the actin–DNAse I complex (Kabsch et al., 1990), the loop at its base extends outward from the surface of the protein. It then hooks back in toward the surface placing the four residues

of the hydrophobic plug in an orientation pointed away from the solvent towards Tyr188. In this conformation, the plug residues would not be oriented properly to interact with actin subunits on the adjacent strand. In the model F-actin structure, the top half of the loop has rotated so that the entire loop points away from the surface of the protein allowing the plug–pocket interaction to occur. If this model is correct, substitution of aspartic acid for leucine at position 266 might increase the hydrophilic character of the plug enough to allow the loop in G-actin to extend into the solvent instead of bending back toward the protein surface. Although our work suggests the $L_{266}D$ mutation causes small conformation changes in the monomer, we have no explicit evidence that these changes represent movement of the loop.

The ratio of the monomers in each of these conformations may affect the rates at which nucleation and elongation occur. Since nucleation is the slower of the two processes, one would predict that the favored conformation for the loop in G-actin is the hook form. We hypothesize that once a nucleus has formed, the interaction of a new monomer with the nucleus causes a change in the loop, in effect shifting the equilibrium position for its conformation toward the extended position thereby facilitating monomer addition to the growing filament.

The relatively minimal effects observed with the $L_{266}D$ actin in vivo do not reflect the magnitude of the effects on nucleation and polymer formation observed in vitro. Two possible explanations can be offered for this apparent paradox. First, at 10°C, when only about a 40% increase in generation time is observed compared with wild-type cells, other processes within the cell may become more rate limiting for growth than the disruption of actin polymerization thus masking the effect of the mutation. Second, although spontaneous nucleation of actin filament formation and filament elongation in vitro are severely affected at 10°C, addition of pre-formed nuclei resulted in a greatly enhanced rate of polymer formation. Furthermore, at 4°C, where not even the addition of seeds induced the formation of stable filaments, such filaments were observed in the presence of phalloidin which is thought to provide cross-strand stability. It is unlikely that spontaneous nucleation of actin polymerization in the cell is required to any great extent. A number of known actin binding proteins can nucleate filament formation, and proteins such as tropomyosin can stabilize filaments once they have formed (Stossel et al., 1985). Proteins similar to these probably direct the deposition of actin filaments in vivo, thereby overcoming the most drastic effects of the $L_{266}D$ mutation.

Shutt et al. (1989), based on their work with the crystal structure of the actin/profilin complex, have suggested a possible alternative model for the actin filament. In this ribbon structure, the small domain consisting of subdomains 1 and 2 is in the interior of the filament where subdomain 2 contacts the small domain of one neighboring monomer and the top of the large domain (subdomain 4) of another monomer. The interface between subdomains 3 and 4 where the hydrophobic loop is located is on the exterior of the filament, apparently not involved directly in intersubunit contacts. For our results to be consistent with this model, one would have to postulate that alteration of the loop by the $L_{266}D$ mutation produced conformational changes in subdomains 2 and/or 4 large enough to cause filament disruption. Although this mutation does produce conformation changes in the monomer, the effects on the monomer observed suggest that these changes are minimal. Thus, although our results do not contradict the Shutt model, we believe that the behavior of the $L_{266}D$ mutant actin is more in agreement with the prediction of Holmes' model for F-actin.

Our work represents the first experimental test of the part of the Holmes model involving the hydrophobic plug. Although our results are consistent with the predictions of this model, they do not prove it. Proof must await a further characterization of the switch in loop conformations and an actual demonstration of an interaction between the hydrophobic plug and the pocket in the actin filament.

We thank Gregory DeKoster and Charles Swenson for their assistance with the circular dichroism and light scattering measurements. We would also like to thank Jeff Kavanaugh for his considerable help in generating Fig. 1, *A* and *B* and John Cooper for providing us with Fig. 1 *C*. Light scattering and circular dichroism measurements were performed on instruments in the University of Iowa Protein Structure Facility. We would also like to thank Kathy Walters and Laura Rain of the University of Iowa Central Electron Microscopy Facility for their help.

Supported in part by a grant to P. A. Rubenstein from the National Institutes of Health (GM-33689) and by fellowships to X. Chen and R. K. Cook from the Iowa Affiliate of the American Heart Association.

Received for publication 14 January 1993 and in revised form 31 August 1993.

References

Abola, E. E., F. C. Bernstein, S. H. Bryant, T. F. Koetzle, and J. Weng. 1987. Protein Data Bank. *In* Crystallographic Databases–Information Content, Software Systems, Scientific Applications. F. H. Allen, G. Bergerhoff, and R. Sievers, editors. Data Commission of the International Union of Crystallography. Bonn/Cambridge/Chester. 107–132.

Ausubel, F. M., R. Brent, R. E. Kingston, D. D. Moore, J. A. Smith, J. B. Seidman, and K. Struhl. 1987. Current Protocols in Molecular Biology. John Wiley & Sons, NY.

Baldwin, R. L. 1986. Temperature dependence of the hydrophobic interaction in protein folding. *Proc. Natl. Acad. Sci. USA.* 83:8069–8072.

Bernstein, F. C., T. F. Koetzle, G. J. B. Williams, E. F. Meyer, Jr., M. D. Brice, J. R. Rodgers, O. Kennard, T. Shimanouchi, and M. Tasumi. 1977. The protein data bank: a computer-based archival file for macromolecular structures. *J. Mol. Biol.* 112:535–542.

Bertazzon, A., G. H. Tian, A. Lamblin, and T. Y. Tsong. 1990. Enthalpic and entropic contributions to actin stability: Calorimetry, circular dichroism, and fluorescence study and effects of calcium. *Biochemistry.* 29:291–298.

Bremer, A., and U. Aebi. 1992. The structure of the F-actin filament and the actin molecule. *Curr. Opin. Cell Biol.* 4:20–26.

Bremer, A., R. C. Millonig, R. Sutterlin, A. Engel, T. D. Pollard, and U. Aebi. 1991. The structural basis for the intrinsic disorder of the F-actin filament: the lateral slipping model. *J. Cell Biol.* 115:689–703.

Chowdhury, S., K. W. Smith, and M. C. Gustin. 1992. Osmotic stress and the yeast cytoskeleton: phenotype-specific suppression of an actin mutation. *J. Cell Biol.* 118:561–571.

Cook, R. K., W. T. Blake, and P. A. Rubenstein. 1992. Removal of the amino-terminal acidic residues of yeast actin. *J. Biol. Chem.* 267:9430–9436.

Cook, R. K., D. Root, C. Miller, E. Reisler, and P. A. Rubenstein. 1993. Enhanced stimulation of myosin subfragment 1 ATPase activity by addition of negatively charged residues to the yeast actin NH2-terminus. *J. Biol. Chem.* 268:2410–2415.

Cook, R. K., and P. A. Rubenstein. 1992. The generation and isolation of mutant actins. *In* The Cytoskeleton: A Practical Approach. K. L. Carraway and C. A. C. Carraway, editors. Oxford University Press, New York. 99–122.

Cook, R. K., D. R. Sheff, and P. A. Rubenstein. 1991. Unusual metabolism of the yeast actin amino terminus. *J. Biol. Chem.* 266:16825–16833.

Cooper, J. 1992. Actin filament assembly and organization in vitro. *In* The Cytoskeleton: A Practical Approach. K. L. Carraway and C. A. C. Carraway, editors. Oxford University Press, New York. 47–71.

Elzinga, M., J. H. Collins, W. N. Kuehl, and R. S. Adelstein. 1973. Complete amino acid sequence of actin of rabbit skeletal muscle. *Proc. Natl. Acad. Sci. USA.* 70:2687–2691.

Frieden, C. 1982. The Mg+2 induced conformational change in rabbit skeletal muscle G-actin. *J. Biol. Chem.* 257:2882–2886.

Gallwitz, D., and I. Sures. 1980. Structure of a split gene: complete nucleotide sequence of the actin gene in *Saccharomyces cerevisiae*. *Proc. Natl. Acad. Sci. USA.* 77:2546–2550.

Haarer, B. K., S. H. Lillie, A. E. M. Adams, V. Magdolen, W. Bandlow, and S. S. Brown. 1990. Purification of profilin from *Saccharomyces cerevisiae* and analysis of profilin-deficient cells. *J. Cell Biol.* 110:105–114.

Holmes, K. C., D. Popp, W. Gebhard, and W. Kabsch. 1990. Atomic model of the actin filament. *Nature (Lond.).* 347:44–49.

Ito, H., Y. Fukuda, K. Murata, and A. Kimura. 1983. Transformation of intact yeast cells treated with alkali cations. *J. Bacteriol.* 153:163–168.

Johnson, M. L., and S. G. Frasier. 1985. Nonlinear least-squares analysis. *Methods Enzymol.* 117:301–342.

Kabsch, W., H. G. Mannherz, D. Suck, E. Pai, and K. C. Holmes. 1990. Atomic structure of the actin: DNAseI complex. *Nature (Lond.).* 347:37–44.

Lorenz, M., D. Popp, and K. C. Holmes. 1993. Refinement of the F-actin model against X-ray fiber diffraction data by the use of a directed mutation algorithm. *J. Mol. Biol.* In press.

Milligan, R. A., M. Whittaker, and D. Safer. 1990. Molecular structure of F-actin and location of surface binding sites. *Nature (Lond.).* 348:217–221.

Mockrin, S. C., and E. D. Korn. 1980. *Acanthamoeba* profilin interacts with G-actin to increase the rate of exchange of actin bound adenosine 5′-triphosphate. *Biochemistry.* 19:5359–5362.

Ng, R., and J. Abelson. 1980. Isolation and sequence of the gene for actin in Saccharomyces cerevisiae. *Proc. Natl. Acad. Sci. USA.* 77:3912–3916.

Pardee, J. D., and J. A. Spudich. 1982. Purification of muscle actin. *Methods Enzymol.* 85:164–181.

Pringle, J. R., A. E. M. Adams, D. G. Drubin, and B. K. Haarer. 1991. Immunofluorescence methods for yeast. *Methods Enzymol.* 194:565–601.

Privalov, P. L., and S. J. Gill. 1988. Stability of protein structure and hydrophobic interaction. *Adv. Prot. Chem.* 39:191–234.

Schutt, C. E., U. Lindberg, J. Myslik, and N. Strauss. 1989. Molecular packing in profilin: actin crystals and its implications. *J. Mol. Biol.* 209:735–746.

Sherman, F. 1990. Getting started with yeast. *Methods Enzymol.* 194:3–20.

Spudich, J. 1974. Biochemical and structural studies of actomyosin-like proteins from non-muscle cells. II. Purification, properties, and membrane association of actin from amoebae of *Dictyostelium discoideum*. *J. Biol. Chem.* 249:6013–6020.

Stossel, T., C. Chaponnier, R. Ezzel, J. Hartwig, P. Janmey, D. Kwiatkowski, S. Lind, D. Smith, F. Southwick, H. Yin, and K. Zaner. 1985. Nonmuscle actin-binding proteins. *Annu. Rev. Cell Biol.* 1:353–402.

Strezelecka-Golaszewska, H., Y. Venyaminov, S. Zmorzynski, and M. Mossakowska. 1985. Effects of various amino acid replacements on the conformational stability of G-actin. *Eur. J. Biochem.* 147:331–342.

Tobacman, L. S., and E. D. Korn. 1982. The regulation of actin polymerization and the inhibition of monomeric actin ATPase activity by Acanthamoeba profilin. *J. Biol. Chem.* 257:4166–4170.

Weeds, A. G., and R. S. Taylor. 1975. Separation of subfragment-1 isoenzymes from rabbit muscle myosin. *Nature (Lond.).* 257:54–56.

Wertman, K. F., D. G. Drubin, and D. Botstein. 1992. Systematic mutational analysis of the yeast ACT1 gene. *Genetics.* 132:337–350.

Zimmerle, C. T., and C. Frieden. 1988. Effect of pH on the mechanisms of actin polymerization. *Biochemistry.* 27:7766–7772.